Liquid Crystals
Publication details, including instructions for authors and subscription information:
http://www.informaworld.com/smpp/title~content=t713926090

The effect of lateral fluoro substituents on the mesomorphic properties of semi-fluorinated chiral liquid crystals

Shune-Long Wu[a]; Cho-Ying Lin[a]
[a] Department of Chemical Engineering, Tatung University, Taipei, 104, Taiwan, ROC

To cite this Article Wu, Shune-Long and Lin, Cho-Ying(2006) 'The effect of lateral fluoro substituents on the mesomorphic properties of semi-fluorinated chiral liquid crystals', Liquid Crystals, 33: 8, 953 — 960
To link to this Article: DOI: 10.1080/02678290600905610
URL: http://dx.doi.org/10.1080/02678290600905610

Liquid Crystals, Vol. 33, No. 8, August 2006, 953–960

The effect of lateral fluoro substituents on the mesomorphic properties of semi-fluorinated chiral liquid crystals

SHUNE-LONG WU* and CHO-YING LIN

Department of Chemical Engineering, Tatung University, 40 Chungshan N. Rd, 3rd Sec., Taipei, 104, Taiwan, ROC

(*Received 20 March 2006; accepted 15 June 2006*)

Two series of semi-fluorinated chiral liquid crystals, 2F(*m*=8–12) and 3F(*m*=8–12), with monofluoro-substitution at the 2- and 3-positions of the first phenyl ring near the chiral chain, respectively, have been synthesized and characterized. The mesomorphic properties were analyzed by differential scanning calorimetry, polarizing optical microscopy and electric-optical measurements. It was found that in the series 2F(*m*=8–12) the two materials 2F(*m*=8, 10) exhibit broad temperature ranges for the antiferroelectric SmC_A^* phase with the phase sequence $\mathrm{SmA}^*-\mathrm{SmC}^*-\mathrm{SmC}_A^*$. In the series 3F(*m*=8–12), the three materials 3F(8–10) display the $\mathrm{SmA}^*-\mathrm{SmC}_A^*$ transition, accompanied by a higher order ferroelectric SmX* (SmI* or SmF*) phase. The remaining materials exhibit SmA* and SmC* phases. The switching current, spontaneous polarization, title angle, dielectric constant and electro-optical response for the materials in the SmC*, SmC_A^* and SmX* phases were measured. The effect of the position of the fluoro substituent and the influence of the alkyl chain length on mesomorphic behaviour are discussed.

1. Introduction

The fluorine atom is generally used in the design of liquid crystal molecules because its presence in a molecule has many interesting effects. For example, some perfluorinated liquid crystal materials with a fluorine atom attached to the molecular tail favour the formation of the smectic phase [1–7] and possess lower viscosity, lower birefringence and higher chemical stability [8–16]. The fluorine atom has also been used as a lateral substituent on the mesogenic core of liquid crystal molecules [17–24]. *Coates*' experimental results demonstrated that the incorporation of a lateral fluorine substituent in the mesogenic core of a molecule causes some degree of steric asymmetry in the bank; it therefore reduces the occurrence of a higher order smectic phase, and in most cases decreases the melting point [25]. Other reports have indicated that the introduction of a lateral fluorine substituent into mesogenic cores can enhance the formation of a tilted smectic C phase [23, 26–27].

Our previous studies on a homologous series of semi-fluorinated chiral liquid crystals, MPFPECP*m*BC-(*m*=8–12), showed that this series of materials has the mesophase sequence $\mathrm{I}-\mathrm{SmA}^*-\mathrm{SmC}^*-\mathrm{SmC}_A^*-\mathrm{Cr}$, with a wide temperature range of the antiferroelectric SmC_A^* phase [28, 29]. In order to explore this field further, two series of chiral liquid crystal materials, 2F(*m*=8–12) and 3F(*m*=8–12), with fluoro substituents at the 2 and 3-positions of the phenyl ring, respectively, were prepared for investigation. The general structural formulas are depicted below. The influences of fluoro-substitution and an achiral alkyl chain on the formation of the antiferroelectric SmC_A^* phase are discussed.

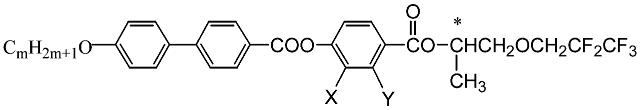

MPFPECPmBC; m=8-12, X=Y=H
2F(m); m=8-12, X=H, Y=F
3F(m); m=8-12, X=F, Y=H

2. Experimental

2.1. *Characterization of the materials*

The chemical structures for intermediates and target materials were analyzed by nuclear magnetic resonance spectroscopy using a Jeol EX-500 FT-NMR spectrometer. The purity was checked by thin layer chromatography and further confirmed by elemental analysis using a Perkin-Elmer 2400 spectrometer. Transition temperatures and phase transition enthalpies of the materials were determined by differential scanning calorimetry using a Perkin-Elmer DSC7 calorimeter at

---

*Corresponding author. Email: slwu@ttu.edu.tw

Liquid Crystals
ISSN 0267-8292 print/ISSN 1366-5855 online © 2006 Taylor & Francis
http://www.tandf.co.uk/journals
DOI: 10.1080/02678290600905610

heating/cooling rates of 5°C min^{-1}. Mesophases were principally identified by microscopic texture of the materials sandwiched between two glass plates under a crossed polarizing microscope using a Nikon Microphot-FXA in conjunction with a Mettler FP82 hot stage.

The physical properties of ferroelectric and antiferroelectric phases for the materials were measured in homogeneously aligned cells purchased from E. H. C. Co. Japan. The spontaneous polarization ($\mathbf{P}_s$) was measured by a triangular wave method [30]. Optical transmittance versus applied electric field was measured using a He-Ne laser (5 mW, 632.8 nm) as a probe beam [31, 32]; this beam passed though a cell between crossed polarizers, whose axes were parallel and perpendicular to the smectic layer normal, and was then detected by a photodiode. The signals were detected using a HP54502A digital oscilloscope. The voltage applied to the cell was produced by an arbitrary wave-form generator (AG1200) and amplified by a homemade power preamplifier.

2.2. *Preparation of materials*

The target materials were prepared by the synthetic procedure sketched in scheme 1. (*S*)-1-Methyl-2-(2,2,3,3,3-pentafluoropropyloxy)ethanol was prepared by reacting (*S*)-propylene oxide with 2, 2, 3, 3, 3-pentafluoro-1-propanol as described before [29]. Thin layer chromatography was performed with TLC sheets coated with silica; spots were detected by UV irradiation. Silica gel (MN kieselgel 60, 70–230 mesh) was used for column chromatography. Anhydrous organic solvents, dichloromethane (CH_2Cl_2) and tetrahydrofuran (THF), were purified by treatment with CaH_2 and $LiAlH_4$, respectively, and distilled before use. The detailed procedures for the syntheses of the materials, 2F(*m*=8–12) and 3F(*m*=8–12), are described as follows.

2.2.1. 2-Fluoro-4-methoxycarbonyloxybenzoic acid, I(2F). 2-Fluoro-4-methoxycarbonyloxybenzoic acid was prepared following a method reported in the literature [33, 34]. ^1H NMR (500 MHz, DMSO-d_6): δ(ppm) 3.84–3.87 (s, 3H, $-OCH_3$), 7.16–7.23 (d, 1H,

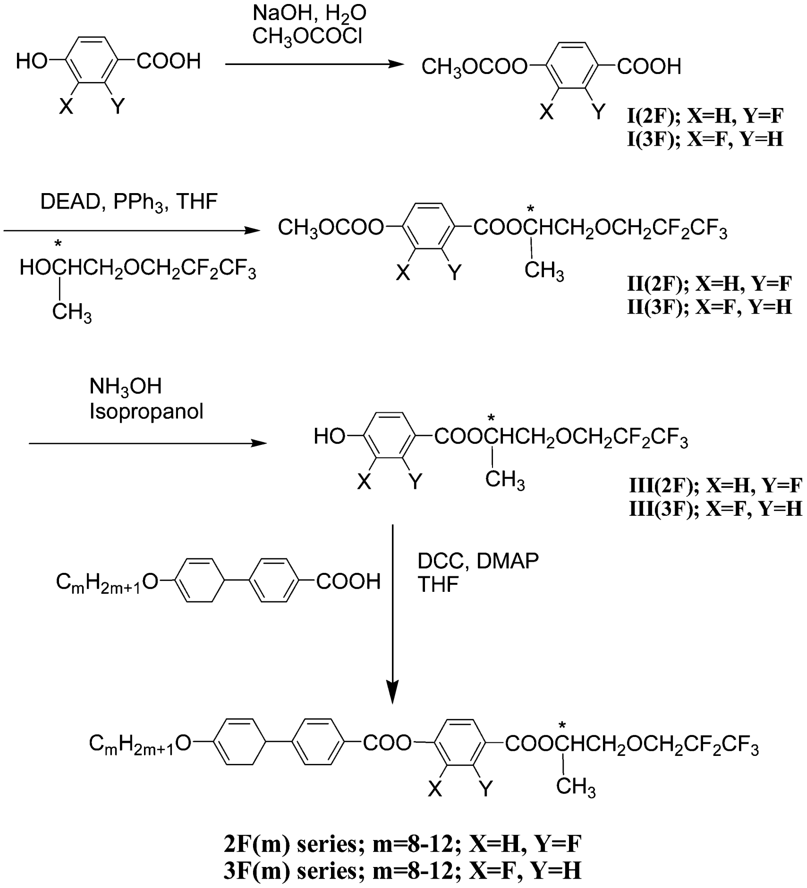

Scheme 1. Schematic procedures for the synthesis of the chiral materials 2F(*m*=8–12), 3F(*m*=8–12).

–Ar**H** J=6.7 Hz), 7.31–7.38 (d, 1H, –Ar**H**, J=9.4 Hz), 7.91–7.95 (t, 1H, –Ar**H**, J=8.5 Hz), 9.15 (s, 1H, –COO**H**).

2.2.2. 3-Fluoro-4-methoxycarbonyloxybenzoic acid, I(3F). 3-Fluoro-4-methoxycarbonyloxybenzoic acid was prepared following a previously reported method [35–38]. ^{1}H NMR (500 MHz, DMSO-d_6): δ(ppm) 3.96 (s, 3H, –OC**H**$_3$), 7.34–7.37 (t, 1H, –Ar**H** J=7.4 Hz), 7.91–7.93 (d, 1H, –Ar**H**, J=9.8 Hz), 7.93–7.94 (t, 1H, –Ar**H**, J=6.1 Hz), 9.03 (s, 1H, –COO**H**).

2.2.3. (*R*)-1-Methyl-2-(2,2,3,3,3-pentafluoropropyloxy)-ethyl 2-fluoro-4-(methoxycarbonyloxy)benzoate, II(2F). A solution of diethyl azodicarboxylate (DEAD, 1.7 g, 9.9 mmol) and material I(2F) (2.1 g, 9.9 mmol) in anhydrous THF (12 ml) was added dropwise to a solution of triphenylphosphine (Ph_3P, 2.6 g, 9.9 mmol) and (*S*)-1-methyl-2-(2,2,3,3,3-pentafluoropropyloxy)-ethanol (1.27 g, 9 mmol) in anhydrous THF (12 ml) at room temperature with vigorous stirring; the reaction soon started. After standing the mixture overnight at room temperature, triphenylphosphine oxide was removed by filtration; THF was then removed under vacuum. The product was isolated by column chromatography over silica gel (70–230 mesh) using ethyl acetate/hexane (v/v=1/4) as eluant to give a colourless liquid. A 65% yield of material II(2F) was obtained. ^{1}H NMR (500 MHz, $CDCl_3$): δ(ppm) 1.36–1.60 (d, 3H, –CH*C**H**$_3$, J=8.4 Hz), 3.75–3.96 (m, 2H, –CH*C**H**$_2$OCH$_2$–), 3.92–3.93 (s, 3H, –OCOOC**H**$_3$, J=6.5 Hz), 3.95–3.98 (m, 2H, –CH$_2$OC**H**$_2$CF$_2$–), 5.29–5.36 (m, 1H, –COOC**H***CH$_3$), 7.25–7.27 (d, 2H, Ar**H**, J=8.8 Hz), 8.05–8.08 (t, 1H, Ar**H**, J=8.7 Hz).

2.2.4. (*R*)-1-Methyl-2-(2,2,3,3,3-pentafluoropropyloxy)-ethyl 3-fluoro-4-(methoxycarbonyloxy]benzoate, II(3F). This material was prepared in an analogous manner to II(2F); the yield was 56%. ^{1}H NMR (500 MHz, $CDCl_3$): δ(ppm) 1.37–1.60 (d, 3H, –CH*C**H**$_3$, J=8.2 Hz) 3.96 (s, 3H, –OC**H**$_3$), 5.28–5.37 (m, 1H, –COOC**H***CH$_3$) 7.34–7.37 (t, 1H, –Ar**H**, J=7.4 Hz), 7.91–7.93 (d, 1H, –Ar**H**, J=8.8 Hz).

2.2.5. (*R*)-1-Methyl-2-(2,2,3,3,3-pentafluoropropyloxy)-ethyl 2-fluoro-4-hydroxybenzoate, III(2F). Material II(2F) (1.2 g, 3mmol) was stirred in a mixture of isopropanol (90 ml) and aqueous ammonia (28%, 30 ml) at room temperature for 50 min (TLC analysis showed complete reaction) and then poured into water (40 ml) with stirring. The product was extracted using dichloromethane (3 × 50 ml). The combined organic extracts were washed with brine (3 × 50 ml), dried ($MgSO_4$), filtered and evaporated to give a colourless oil. The oil was purified by column chromatography over silica gel (70–230 mesh) using dichloromethane as eluant. The resulting oil was dried in vacuo; an 80% yield of material III(2F) was obtained and identified by ^{1}H NMR. ^{1}H NMR (500 MHz, $CDCl_3$): δ(ppm) 1.34–1.37 (d, 3H, –CH*C**H**$_3$, J=6.2 Hz), 3.89–3.95 (m, 2H, –CH*C**H**$_2$OCH$_2$–), 3.95–4.04 (m, 2H, –CH$_2$ OC**H**$_2$CF$_2$–), 5.24–5.32 (m, 1H, –COOC**H***CH$_3$), 5.92 (s, 1H, –O**H**,), 6.57–6.63 (d, 1H, Ar**H**, J=11.4 Hz), 6.64–6.68 (d, 1H, Ar**H**, J=8.4 Hz), 7.79–7.87 (t, 1H, Ar**H**, J=8.8 Hz).

2.2.6. (*R*)-1-Methyl-2-(2,2,3,3,3-pentafluoropropyloxy)-ethyl 3-fluoro-4-hydroxybenzoate, II(3F). This material was prepared in an analogous manner to III(2F); the yield was 78%. ^{1}H NMR (500 MHz, $CDCl_3$): δ(ppm) 1.34–1.37 (d, 3H, –CH*C**H**$_3$, J=6.2 Hz), 3.68–3.75 (m, 2H, –CH*C**H**$_2$OCH$_2$–), 3.89–4.03 (m, 2H, –CH$_2$ OC**H**$_2$CF$_2$–), 5.26–5.33 (m, 1H, –COOC**H***CH$_3$), 6.02 (s, 1H, –O**H**,), 6.94–7.03 (t, 1H, Ar**H**, J=8.4 Hz), 7.73–7.78 (d, 2H, Ar**H**, J=10.2 Hz).

2.2.7. (*R*)-2-Fluoro-4-[1-methyl-2-(2,2,3,3,3-pentafluoro-propyloxy)ethyloxycarbonyl]phenyl 4′-alkyloxybiphenyl-4-carboxylates, 2F(*m*=8–12). A mixture of 4-(4′-alkyloxyphenyl)benzoic acid (2.8 mmol), material III(2F) (1.07 g, 3.1 mmol) *N*,*N*′-dicyclohexylcarbodiimide (0.57 g, 2.8 mmol), 4-dimethylaminopyridine (0.05 g, 0.28 mmol) and dry THF (15 ml) was stirred at room temperature for three days. The precipitate was filtrated off and the filtrate washed with 5% aqueous acetate acid (3 × 50 ml), 5% aqueous sodium hydrogen carbonate (3 × 50 ml) and water (3 × 50 ml), dried over anhydrous magnesium sulfate ($MgSO_4$) and concentrated under vacuum. The residue was purified by column chromatography over silica gel (70–230 mesh) using dichloromethane as eluant. After purification by recrystallization from absolute ethanol, a 54–62% yield of final product was obtained. ^{1}H NMR (500 MHz, $CDCl_3$) for 2F(*m*=10) as an example: δ(ppm) 0.87–0.90 (t, 3H, –CH$_2$C**H**$_3$, J=7.0 Hz), 1.25–1.56 (m, 17H, –OCH$_2$CH$_2$(C**H**$_2$)$_7$–, –OCH*C**H**$_3$–), 1.80–1.83 (m, 2H, –OCH$_2$C**H**$_2$–), 3.78–3.80 (m, 2H, –CH*C**H**$_2$O–), 3.99–4.06 (m, 4H, –CH$_2$OC**H**$_2$CF$_2$–, –C**H**$_2$OAr–), 5.31–5.37 (m, 1H, –COOC**H***CH$_3$–) 7.00–7.01 (d, 2H, Ar**H**, J=5.1 Hz), 7.11–7.15 (t, 2H, Ar**H**, J=9.0 Hz), 7.59–7.60 (d, 2H, Ar**H**, J=8.7 Hz), 7.69–7.71 (d, 2H, Ar**H**, J=8.4 Hz), 8.01–8.04 (t, 1H, Ar**H**, J=8.8 Hz), 8.20–8.22 (d, 2H, Ar**H**, J=8.3 Hz).

2.2.8. (*R*)-3-Fluoro-4-[1-methyl-2-(2,2,3,3,3-pentafluoro-propyloxy)ethyloxycarbonyl]phenyl 4′-alkyloxybiphenyl-4-carboxylates, 3F(*m*=8–12). Theses materials were prepared in an analogous manner to 2F(*m*=8–12); the yields were 50–60%. The chemical shifts for material in

^{1}H NMR (500 MHz, $CDCl_3$) for 3F(m=10) as an example: δ(ppm) 0.87–0.90 (t, 3H, $-CH_2\mathbf{CH_3}$, J=6.4 Hz), 1.28–1.55 (m, 17H, $-OCH_2CH_2(\mathbf{CH_2})_7-$, $-OCH^*\mathbf{CH_3}-$), 1.78–1.84 (m, 2H, $-OCH_2\mathbf{CH_2}-$), 3.75–3.82 (m, 2H, $-CH^*\mathbf{CH_2}O-$), 3.91–4.04 (m, 4H, $-CH_2O\mathbf{CH_2}CF_2-$, $-\mathbf{CH_2}OAr-$), 5.30–5.36 (m, 1H, $-COOC\mathbf{H}^*CH_3-$) 7.00–7.01 (d, 2H, Ar**H**, J=8.6 Hz), 7.36–7.39 (t, 1H, Ar**H**, J=7.4 Hz), 7.59–7.60 (d, 2H, Ar**H**, J=8.6 Hz), 7.70–7.71 (d, 2H, Ar**H**, J=8.3 Hz), 7.87–7.91 (t, 2H, Ar**H**, J=8.4 Hz), 8.23–8.25 (d, 2H, Ar**H**, J=8.3 Hz).

All the target materials were analyzed by elemental analysis for purity, with satisfactory results.

3. Results and discussion

The mesophases and their corresponding phase transition temperatures for 2F(m=8–12) and 3F(m=8–12) were determined by texture observation using polarizing optical microscopy and differential scanning calorimetry. The SmA* phase was characterized by the formation of focal-conic texture and the SmC* phase by the formation of striped focal-conic texture. The antiferroelectric SmC$^*_A$ and ferroelectric SmX* (SmF* or SmI*) phases appeared as broken focal-conic texture, and were further identified by switching current measurement. The results for mesophases and corresponding transition temperatures for the target materials are shown in table 1.

In the series 2F(m=8–12) materials, it was found that 2F(m=8) and 2F(m=10) exhibit broad temperature ranges (calc. 125 and 88°C, respectively) of the SmC$^*_A$ phase and have the phase sequence SmA* – SmC* – SmC$^*_A$. However, in the series 3F(m=8–12), a direct SmA* – SmC$^*_A$ transition accompanied by a higher order ferroelectric SmX* phase was found in materials 3F(m=8–10). The remainder have the phase sequence SmA*–SmC*. It is worth noting that the antiferroelectric SmC$^*_A$ phase was reported to occur generally in compounds with alkyl chain length from m=8 to 10 for these materials [39–41]. It is also found that as the fluoro substituent moves from the 2- to the 3-position of the phenyl ring, the mesophase transition temperatures of I–SmA* and SmA* – SmC*/SmC$^*_A$ transitions decrease, suggesting that the 2-fluoro substituent is more sterically shielded and molecular broadening is minimized [42].

The physical properties for the materials were measured in 5 μm homogeneous cells. Figure 1 (a) shows the electrical switching response of 2F(m=8) in a 5 μm thick homogeneous cell under a triangular wave voltage with a field frequency of 20 Hz and amplitude of 5 $V_{p\text{-}p}$. The switching currents display one current peak at 151°C, similar to the behaviour reported for the ferroelectric SmC* phase [43]. Two switching current peaks appeared at 120°C, similar to the normal SmC$^*_A$ phase [43], supporting the existence of an antiferroelectric SmC$^*_A$ phase. In figure 1 (b), 3F(m=8) shows

Table 1. The mesophases, transition temperatures (°C) and associated enthalpy data (kJ mol^{-1}, in square brackets) for the chiral materials 2F(m=8–12) and 3F(m=8–12): recorded by DSC at a cooling rate of 5°C min^{-1}.

Material	I		SmA*		SmC*		SmC$^*_A$		SmX*		Cr	m.p.[a]
2F(m=8)	•	157.8 [8.8]	•	151.3 [0.8]	•	150.4 [b]	•		—	24.4 [3.1]	•	77.3 [28.7]
2F(m=9)	•	150.3 [3.9]	•	146.1 [0.5]	•		—		—	28.2 [17.1]	•	70.8 [22.2]
2F(m=10)	•	144.3 [5.7]	•	140.9 [0.4]	•	125.7 [b]	•		—	37.8 [24.0]	•	76.5 [37.0]
2F(m=11)	•	138.5 [4.5]	•	134.9 [0.2]	•		—		—	52.4 [29.0]	•	75.1 [28.4]
2F(m=12)	•	135.0 [4.3]	•	131.9 [0.8]	•		—		—	49.7 [40.1]	•	81.2 [40.2]
3F(m=8)	•	149.2 [8.6]	•		—	102.4 [b]	•	62.0 [1.4]	•	55.7 [17.2]	•	94.6 [31.0]
3F(m=9)	•	141.3 [6.8]	•		—	110.7 [0.07]	•	70.5 [b]	•	43.2 [9.0]	•	85.5 [26.3]
3F(m=10)	•	134.9 [6.8]	•		—	113.1 [0.2]	•	59.3 [b]	•	35.2 [20.9]	•	76.9 [31.7]
3F(m=11)	•	129.3 [7.5]	•	113.5 [0.2]	•		—		—	44.2 [24.3]	•	88.8 [36.9]
3F(m=12)	•	125.0 [6.3]	•	112.8 [0.3]	•		—		—	57.7 [27.5]	•	87.8 [35.9]

[a] m.p. refers to melting point taken from DSC thermograms recorded at heating rates of 5°C min^{-1}. [b] The enthalpy was too small to be determined by DSC.

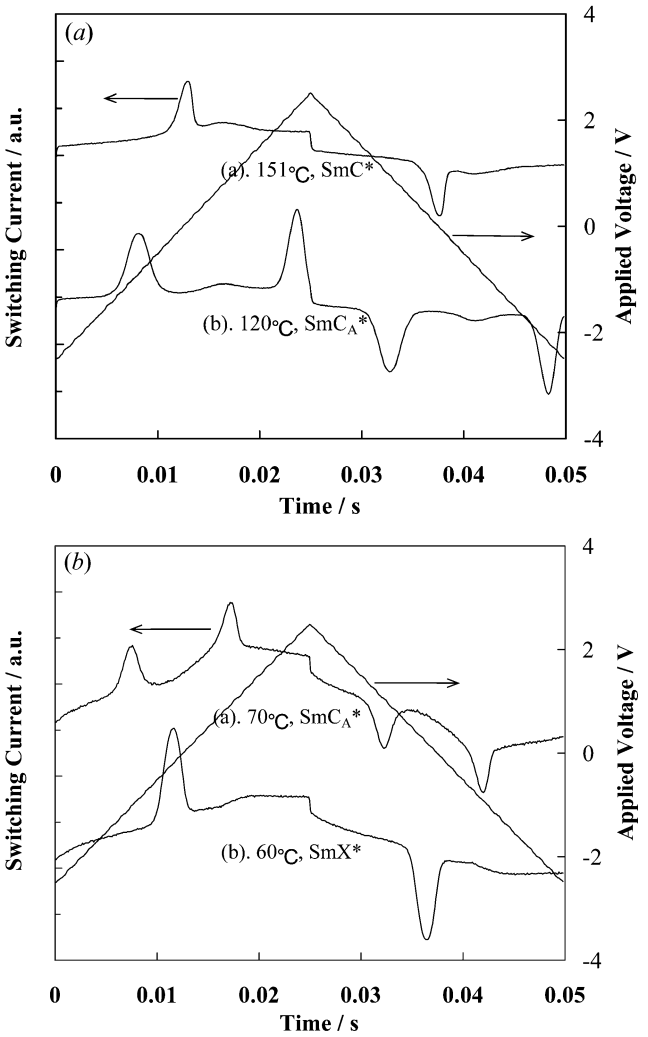

Figure 1. Switching current behaviour of (*a*) 2F(m=8), (*b*) 3F(m=8), obtained at 20 Hz and various temperatures on applying a triangular wave voltage to a in 5 μm thick homogeneously aligned cell.

two current peak at 70°C, indicating an antiferroelectric SmC_A^* phase; but on cooling to 60°C, giving a SmX* phase, a typical ferroelectric single switching peak occurrs. This anomaly was further investigated by the measurement of dielectric constant.

The temperature dependence of the dielectric constant ε' for the chiral materials was measured at 100 Hz in 25 μm homogeneously aligned cells, with the results depicted in figure 2. Figure 2 (*a*) shows the temperature dependence of the dielectric constant ε' of materials 2F(m=8–12). The ε' in the SmA* phase is small; the characteristic point corresponding to the SmA*–SmC* transition is easily seen. The great enhancement of dielectric constant on cooling from SmA* to the SmC* phase is due to the contribution of the Goldstone mode [44]. In the SmC* phase ε' falle to very low values, indicating the formation of the SmC_A^* phase. Figure 2 (*b*) shows the temperature dependence of the dielectric constant ε' of 3F(m=8–12). The dielectric constants are remain very low throughout the SmA* and SmC_A^* phases; however, as the temperature cools from the SmC_A^* to SmX* phase, a large increase in ε' is seen. This demonstrates that the SmX* phase possesses ferroelectric property. Whether this ferroelectric phase is SmI* or SmF*, however, has not been determined at this time.

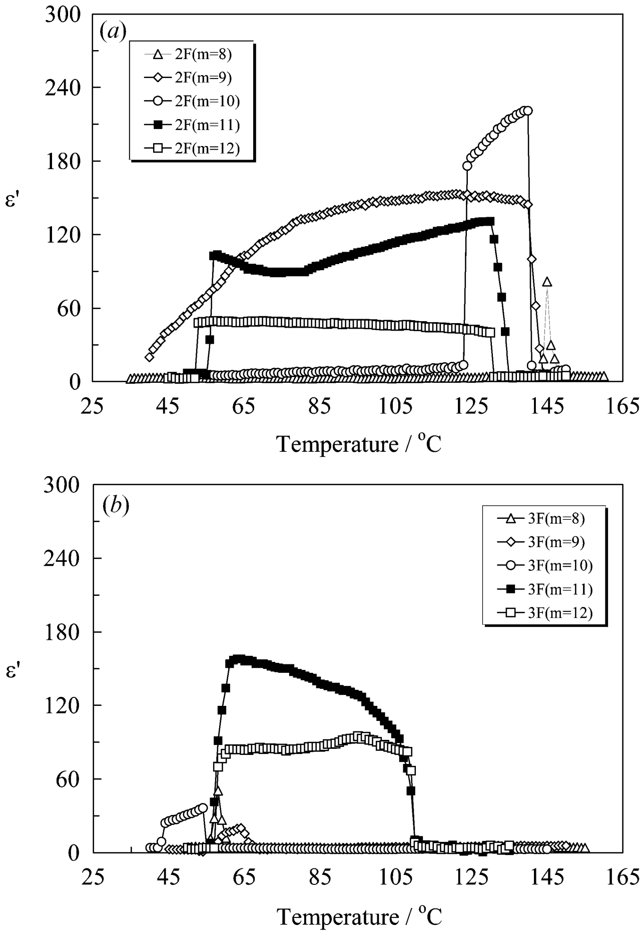

Figure 2. Temperature dependence of dielectric constant ε' for the (*a*) 2F(m=8–12), (*b*) 3F(m=8–12). The measurement was carried out at a cooling rate of 1°C min^{-1} and a frequency of 100 Hz.

Electro-optical responses were obtained under crossed polarizers where the axes of polarizer and analyzer were parallel and perpendicular, respectively, to the smectic layer normal in 5 μm homogeneously aligned cells. Figure 3 illustrates the variation of transmittance with electric field on application of a triangular waveform field measured in the SmC* and SmC_A^* phases for 2F(m=8). As can be seen from figure 3 (*a*), at 151°C and 1 Hz of applied frequency, the

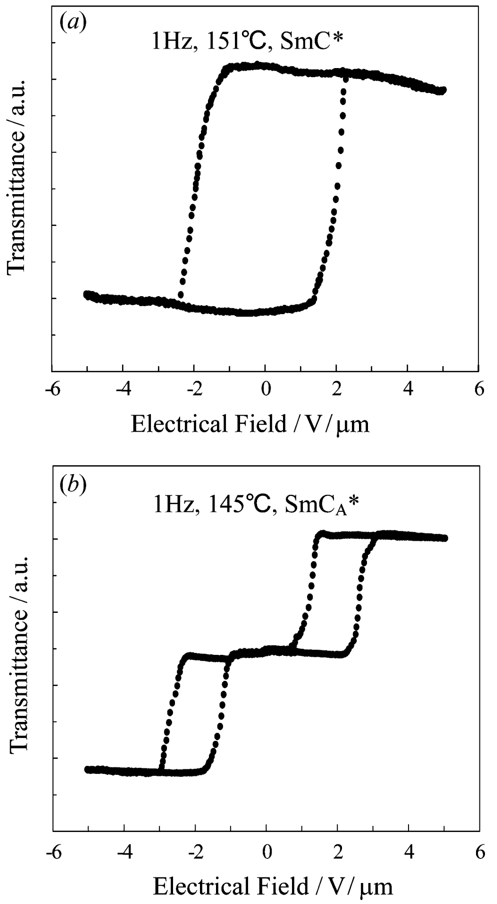

Figure 3. Electro-optical responses of 2F(m=8) (a) in the SmC* phase at 151°C, (b) in the $\mathrm{SmC}_{\mathrm{A}}^{*}$ phase at 145°C and 1 Hz frequency of applgied triangular wave.

curves of transmittance versus applied field display an ideal single hysteresis, representing the existince of the SmC* phase. At 145°C and 1 Hz, the curves of transmittance versus applied field display an ideal double hysteresis, as shown in figure 3 (b), corresponding to tri-stable switching in the antiferroelectric $\mathrm{SmC}_{\mathrm{A}}^{*}$ phase [43].

The temperature dependence of spontaneous polarization (**P**$_s$) of the materials under study is illustrated in figure 4. Figure 4 (a) shows that the measured maximum **P**$_s$ values for 2F(m=9–11), are in the range 101.9–65.4 nC cm^{-2}; figure 4 (b) shows that **P**$_s$ values for 3F(m=9–11) are in range 59.3–49.2 nC cm^{-2}. Figure 4 (c) is a comparison of the maximum **P**$_s$ values for 2F(m=10), 3F(m=10) and the semi-fluorinated material MPFPECP10BC. The order of the **P**$_s$ values for these materials at any temperature below the Curie point is MPFPECP10BC > 2F(m=10) > 3F(m=10), suggesting that the fluoro substituent depresses the polarization of the new materials. This may be due to the compensating effect of the lateral fluoro-substituent with respect to the **P**$_s$. That is, the fluoro substituent points away from the direction of the chiral methyl group, and hence diminishes the observed **P**$_s$ values [45]. In this case, the 2-fluoro substituent has a lower compensating effect than the 3-fluoro substituent.

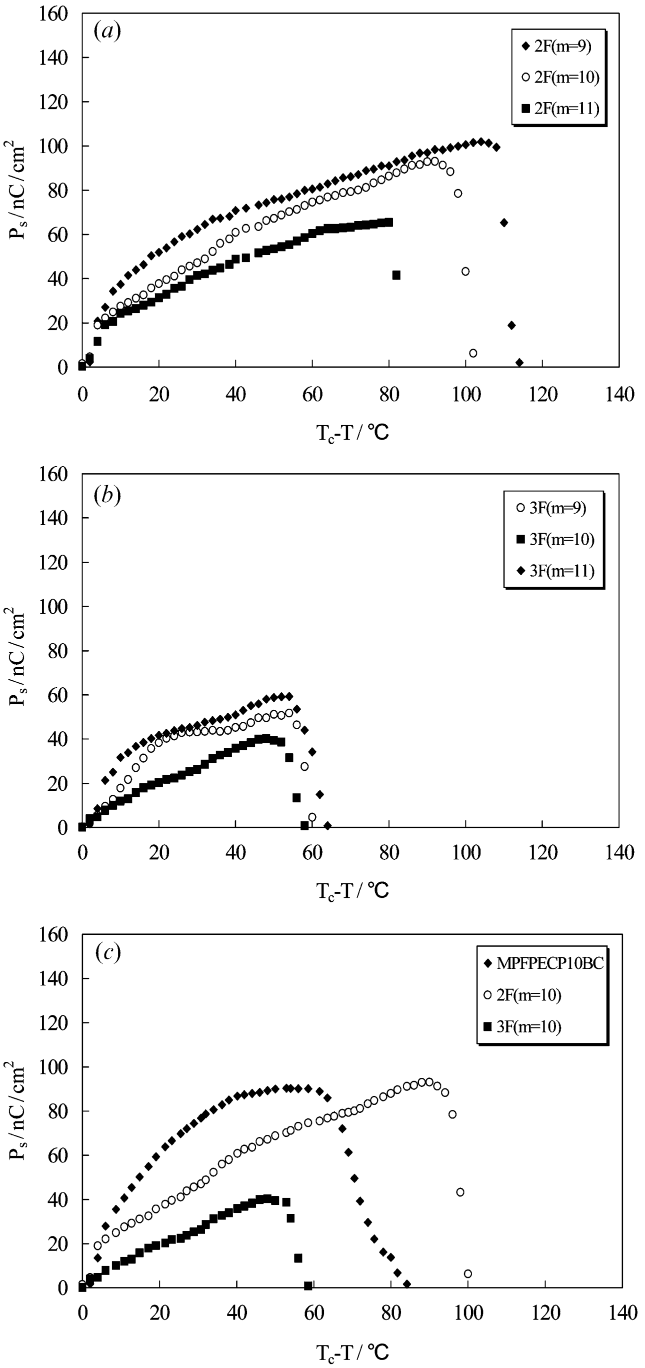

Figure 4. Spontaneous polarization plotted as a function of temperature for (a) 2F(m=9–11), (b) 3F(m=9–11), (c) MPFPECP10BC, 2F(m=10) and 3F(m=10). T_c is the temperature of the SmA*–SmC* transition.

Samples were sandwich-packed in 2 μm thick homogeneously aligned cells for measurement of apparent tilt angle using the usual 2 θ optical method [46]. Figure 5 (*a*) shows that the measured maximum apparent tilt angles for 2F(m=9–11) are in the range 44.6°–41.3°; figure 5 (*b*) shows that for 3F(m=9–11), the values are in the range 33.5–30°. Figure 5 (*c*) is a comparison of the maximum optical title angles for 2F(m=10), 3F(m=10) and MPFPECP10BC. The order of the maximum title angles for these three materials is 2F(m=10) > 3F(m=10) > MPFPECP10BC, suggesting that fluoro substitent in general enhances the apparent title angle. In this case, 2-fluoro-substitution has a larger effect than 3-fluoro-substitution.

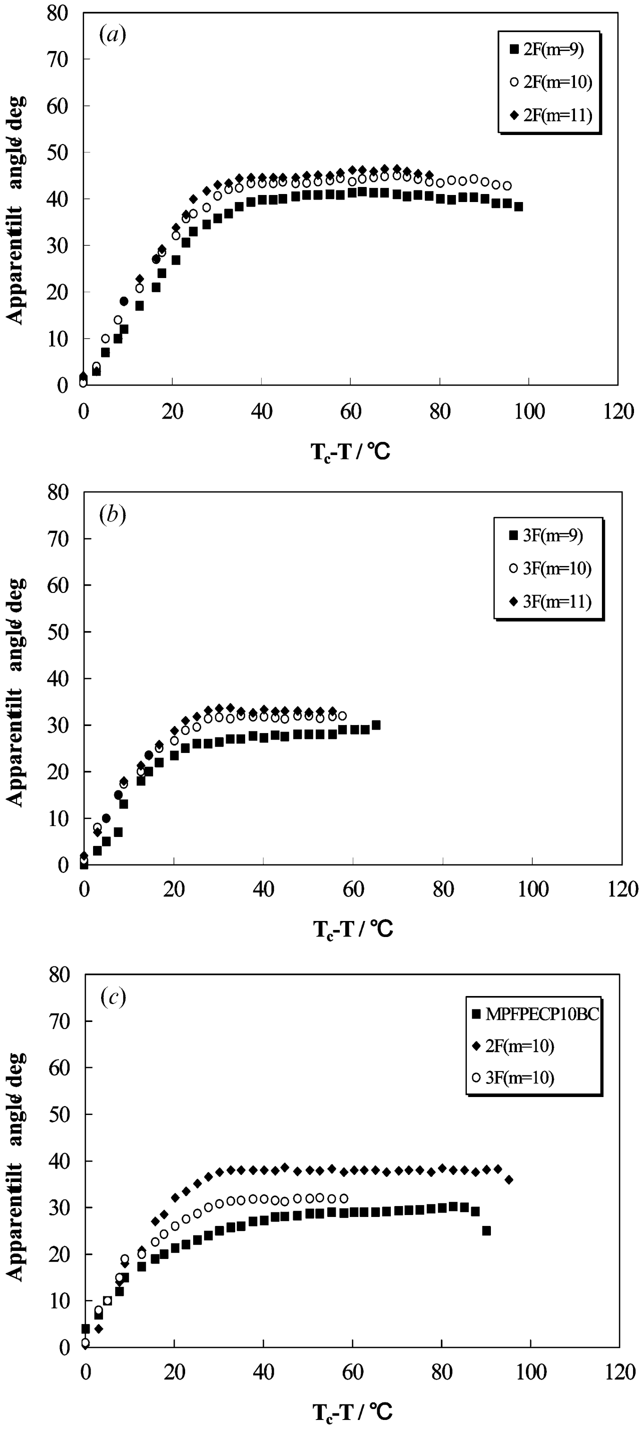

Figure 5. Temperature dependence of apparent tilt angle for (*a*) 2F(m=9–11), (*b*) 3F(m=9–11) and (*c*) MPFPECP10BC, 2F(m=10) and 3F(m=10).

4. Conclusion

Two series of laterally fluoro-subsitituted semi-fluorinated chiral liquid crystal materials derived from (*S*)-1-methyl-2-(2,2,3,3,3-pentafluoropropyloxy)ethanol have been demonstrated to possess ferroelectric SmC* and antiferroelectric SmC_A^* phases. Unlike the semi-fluoro-substituted materials, MPFPECP*m*BC(m=8–10), which show an antiferroelectric phase for all alkyl chain members of the series, fluoro-substitution at the 2- or 3-positions of the phenyl ring seems to suppress the formation of the antiferroelectric phase in longer alkyl chain members of the new materials. Fluoro-substitution in these materials decreases the spontaneous polarization but enhances the apparent tilt angle.

Acknowledgment

The authors are grateful for the financial support of the National Science Council of Taiwan, ROC (NSC 93-2216-E-036-021).

References

[1] S. Takenaka. *Chem. Commun.*, 1748 (1992).
[2] H. Okamoto, H. Murai, S. Takenaka. *Bull. chem. Soc. Jpn.*, **70**, 3163 (1997).
[3] H. Okamoto, N. Yamada, S. Takenaka. *J. Fluorine Chem.*, **91**, 125 (1998).
[4] M. Duan, H. Okamoto, V.F. Petrov, S. Takenaka. *Bull. chem. Soc. Jpn.*, **71**, 2735 (1998).
[5] M. Duan, H. Okamoto, V.F. Petrov, S. Takenaka. *Bull. chem. Soc. Jpn.*, **72**, 1637 (1999).
[6] G. Johansson, V. Percec, G. Ungar, K. Smith. *Chem. Mater.*, **9**, 164 (1997).
[7] G. Fornasieri, F. Guittard, S. Géribaldi. *Liq. Cryst.*, **30**, 663 (2003).
[8] H.T. Nguyen, G. Sigaud, M.F. Achard, F. Hardouin, R.J. Twieg, K. Betterton. *Liq. Cryst.*, **10**, 389 (1991).
[9] P. Kromm, M. Cotrait, H.T. Nguyen. *Liq. Cryst.*, **21**, 95 (1996).
[10] P. Kromm, M. Cotrait, J.C. Rouillon, P. Barois, H.T. Nguyen. *Liq. Cryst.*, **21**, 121 (1996).
[11] H. Liu, H. Nohira. *Liq. Cryst.*, **20**, 581 (1996).
[12] H. Liu, H. Nohira. *Liq. Cryst.*, **22**, 217 (1997).
[13] H. Liu, H. Nohira. *Liq. Cryst.*, **24**, 719 (1998).

[14] E.T. de Givenchy, F. Guittard, F. Bracon, A. Cambon. *Liq. Cryst.*, **26**, 1163 (1999).

[15] E.T. de Givenchy, F. Guittard, F. Bracon, A. Cambon. *Liq. Cryst.*, **26**, 1371 (1999).

[16] H.T. Nguyen, J.C. Rouillon, A. Babeau, J.P. Marcerou, G. Sigaud, M. Cotrait, H. Allouchi. *Liq. Cryst.*, **26**, 1007 (1999).

[17] V. Faye, C. Rouillon, C. Destrade, H.T. Nguyen. *Liq. Cryst.*, **19**, 47 (1995).

[18] C.D. Cruz, J.C. Rouillon, J.P. Marcerou, N. Isaert, H.T. Nguyen. *Liq. Cryst.*, **28**, 125 (2001).

[19] C.D. Cruz, J.C. Rouillon, J.P. Marcerou, N. Isaert, H.T. Nguyen. *Liq. Cryst.*, **28**, 1185 (2001).

[20] S. Essid, M. Manai, A. Gharbi, J.P. Marcerou, J.C. Rouillon, H.T. Nguyen. *Liq. Cryst.*, **31**, 1185 (2004).

[21] C.J. Booth, D.A. Dunmur, J.W. Goodby, J.S. Kang, K.J. Toyne. *J. mater. Chem.*, **4**, 747 (1994).

[22] C.C. Dong, M. Hird, J.W. Goodby. *Ferroelectrics*, **180**, 245 (1996).

[23] C.S. Hsu, C.H. Tsai. *Liq. Cryst.*, **22**, 669 (1997).

[24] S.L. Wu, C.Y. Lin. *Liq. Cryst.*, **30**, 471 (2003).

[25] D. Coates. *Liq. Cryst.*, **2**, 423 (1987).

[26] J.P. LePesant, J.N. Perbert, B. Mouret, M. Hareng, G. Decobert, J.C. Dubois. *Mol. Cryst. liq. Cryst.*, **129**, 61 (1985).

[27] S.M. Kelly. *Liq. Cryst.*, **2**, 423 (1989).

[28] S.L. Wu, C.Y. Lin. *Liq. Cryst.*, **32**, 663 (2005).

[29] S.L. Wu, C.Y. Lin. *Liq. Cryst.*, **32**, 1053 (2005).

[30] K. Miyasato, S. Abe, H. Takezoe, A. Fukuda, E. Kuze. *Jpn. J. appl. Phys.*, **22**, L661 (1983).

[31] A.D.L. Chandani, T. Hagiwara, Y. Suzuki, Y. Ouchi, H. Takazoe, A. Fukuda. *Jpn. J. appl. Phys.*, **27**, L729 (1988).

[32] J. Lee, A.D. Chandani, K. Itoh, Y. Ouchi, H. Takezoe, A. Fukuda. *Jpn. J. appl. Phys.*, **29**, 1122 (1990).

[33] S.L. Wu, C.Y. Lin. *Liq. Cryst.*, **30**, 205 (2003).

[34] S.L. Wu, W.J. Hsieh. *U.S. Pat. Appl. Publ.*, 19 (2004).

[35] B. Kosata, J. Svoboda, V. Novotna, M. Glogarova. *Liq. Cryst.*, **31**, 1367 (2004).

[36] J.W. Goodby, P. Styring, C. Loubser, P.L. Wessels. *Brit. UK Pat. Appl.*, 77 (1994).

[37] C. Loubser, P.L. Wessels, P. Styring, J.W. Goodby. *J. mater. Chem.*, **4**, 71 (1994).

[38] M. Wand, R.R. Vohra, D. Walba. *PCT Int. Appl.*, 50 (1992).

[39] R.P. Tuffin, J.W. Goodby, D. Bennemann, G. Heppke, D. Lötzsch, G. Scherowsky. *Mol. Cryst. liq. Cryst.*, **260**, 51 (1995).

[40] J.W. Goodby, J.S. Patel, E. Chin. *J. mater. Chem.*, **2**, 197 (1992).

[41] T. Fütterer, G. Heppke, D. Lötzsch, D. Moro, J.W. Goodby, R.P. Tuffin. *Liq. Cryst.*, **29**, 1161 (2002).

[42] P.J. Collings, M. Hird. *Introduction to Liquid Crystals Chemistry and Physics*, 70 (1998).

[43] A. Fukuda, Y. Takanishi, T. Isozaki, K. Ishikawa, H. Takezoe. *J. mater. Chem.*, **4**, 997 (1994).

[44] F. Gouda, K. Skarp, S.T. Lagerwall. *Ferroelectrics*, **113**, 165 (1991).

[45] D.D. Parghi, S.M. Kelly, J.W. Goodby. *Mol. Cryst. liq. Cryst.*, **332**, 313 (1999).

[46] K. Terashima, M. Ichihashi, M. Kikuchi, K. Furukawa, T. Inukal. *Mol. Cryst. liq. Cryst.*, **141**, 237 (1986).